Interatomic coulombic decay - the mechanism for rapid deexcitation of hollow atoms

Wilhelm, R. A.; Gruber, E.; Schwestka, J.; Kozubek, R.; Madeira, T. I.; Marques, J. P.; Kobus, J.; Krasheninnikov, A. V.; Schleberger, M.; Aumayr, F.;

Originally published:

September 2017

Physical Review Letters 119(2017)10, 103401

DOI: https://doi.org/10.1103/PhysRevLett.119.103401

Interatomic coulombic decay - the mechanism for rapid de-excitation of hollow atoms

Richard A. Wilhelm,[1,2,*] Elisabeth Gruber,[1] Janine Schwestka,[1] Roland Kozubek,[3] Teresa I. Madeira,[2] José P. Marques,[4] Jacek Kobus,[5] Arkady V. Krasheninnikov,[2] Marika Schleberger,[3] and Friedrich Aumayr[1]

[1] *TU Wien, Institute of Applied Physics, Wiedner Hauptstr. 8-10, 1040 Vienna, Austria, EU*
[2] *Helmholtz-Zentrum Dresden-Rossendorf, Institute of Ion Beam Physics and Materials Research, Bautzner Landstr. 400, 01328 Dresden, Germany, EU*
[3] *University Duisburg-Essen, Faculty of Physics and CENIDE, Lotharstr. 1, 47048 Duisburg, Germany, EU*
[4] *BioISI - Biosystems & Integrative Sciences Institute, Faculdade de Ciências da Universidade de Lisboa, 1749-016 Lisbon, Portugal, EU*
[5] *Nicolaus Copernicus University, Faculty of Physics, Astronomy and Informatics, Institute of Physics, Grudziądzka 5, 87-100 Toruń, Poland, EU*

(Dated: August 15, 2017)

The impact of highly charged ions onto a solid gives rise to charge exchange between the ions and target atoms, so that slow ions get neutralized in the vicinity of the surface. Using highly charged Ar and Xe ions and the surface-only material graphene as a target, we show that the neutralization and de-excitation of the ions proceeds on a sub-10 fs time scale. We further demonstrate that a multiple interatomic coulombic decay (ICD) model of highly charged ions can describe the observed ultrafast de-excitation. Other de-excitation mechanisms involving non-radiative decay and quasi-molecular orbitals formation during the impact are not important, as follows from the comparison of our experimental data with the results of first-principles calculations. Our method also enables the estimation of ICD rates directly.

PACS numbers: 34.35.+a, 34.50.Bw, 34.70.+e, 68.49.Sf, 68.65.-k, 79.20.Rf
Keywords: slow highly charged ion, HCI, graphene, interatomic coulombic decay, ICD

The interaction of ions with solid surfaces involves a variety of different physical processes, as e.g. elastic scattering and the formation of a scattering cascade or inelastic scattering and associated electronic excitations. Both elastic and inelastic scattering of ions may lead to sputtering [1], nano-melting [2], interface mixing [3] and many more observable target modifications [4]. Depending on ion velocity, one of the scattering mechanisms dominates, i.e. for slow ions with $v \ll v_0$ (v_0: Bohr velocity) elastic scattering is the dominant energy loss mechanism. However, in special cases the picture may change. Especially highly charged ions (HCI) have a large inelastic scattering cross section [5], and they deposit their potential energy (total ionization potential) at a shallow layer at the surface. A significant amount of energy - up to some ten keV - is transferred to the target electronic system even when the HCI has a low velocity [6]. For more than 20 years there exists a generally accepted model for neutralization and de-excitation of highly charged ions, which is explained in detail e.g. by Arnau *et al.* [6]. Our findings presented in this manuscript indicate that the current model of hollow atom formation and de-excitation has to be refined. Experimental indications that the modeled de-excitation cascade to the ground state is too slow (bottleneck problem), existed before [7–11], but were misinterpreted by ad-hoc assumptions of enhanced auto-ionization rates or so-called side-feeding processes. In our work we deliberately use a very asymmetric projectile-target combination, namely Xe-C to exclude side-feeding and corresponding molecular orbital formation. We calculate atomic auto-ionization rates for hollow Xe atoms formed during neutralization and find no enhancement. We use a 2D solid (single layer of graphene) to pinpoint the actual interaction time to a few femtoseconds only and thus exclude the possibility of hollow atom de-excitation in deeper layers of a 3D solid. We conclude that Interatomic Coulombic Decay (ICD), a process, which was not considered so far, is responsible for the observed ultrafast neutralization and de-excitation [12]. Studies of ICD are of great importance to understand biological tissue damage, e.g. under energetic particle irradiation, because the origin of tissue damage lies mainly in slow electron production caused by ICD and their ability to efficiently cleave molecular bonds. ICD is sometimes also called direct Auger de-excitation. The idea was first discussed in [13, 14] and also brought up by Cederbaum *et al.* in 1997 [12]. First experimental observation was done by Marburger *et al.* and Jahnke *et al.* in noble gas clusters and dimers, respectively [15, 16]. We show that ICD can explain the ultrafast de-excitation of HCI and thus that ICD at a solid surface can be probed with HCI.

In the beginning of the neutralization process an approaching HCI extracts electrons from the surface already at a distance of several Ångström by classical-over-barrier transport [6, 17] (see 1(a)). The ion is then almost neutralized, but highly excited, giving rise to the formation of a hollow atom with a total excitation energy of still a few ten keV [18, 19]. After transmission through a thin solid film [7, 9, 20] or after scattering under grazing angles [8] the projectiles are measured in very low or neutral charge states [21]. The excitation energy

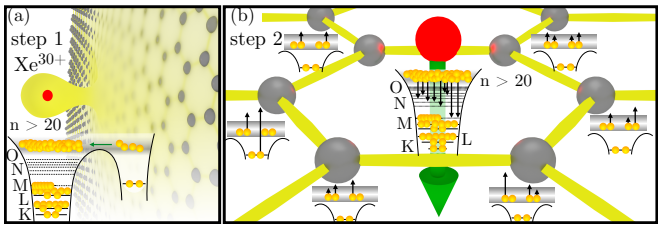

FIG. 1. (color online) (a): Above surface charge capture into highly excited Rydberg states in the ion. A hollow atom is formed. (b): At close distance to the target atoms the hollow atom quenches and releases its excitation energy by excitation/ionization of target electrons via ICD.

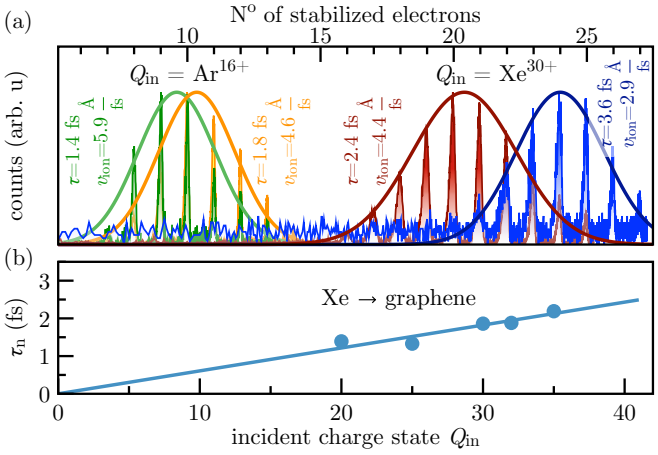

FIG. 2. (color online) (a): Measured number of stabilized electrons for Xe^{30+} and Ar^{16+} ions. The interaction time τ is calculated from the ion velocity v_{ion} and the neutralization length (first capture distance, see SI). (b): Using different kinetic energies and fitting the data with an exponential function a charge neutralization time constant τ_n can be deduced.

must therefore be released by other processes than auto-ionization alone.

In the present work we address the de-excitation dynamics of a hollow atom in the vicinity of a surface. As presented recently by Gruber *et al.* [21] and supplemented by new data here (see fig. 2) a highly charged Xe ion captures and *stabilizes* (not looses electrons due to auto-ionization) up to 27 electrons in less than 4 fs. Measurements with highly charged Ar ions with L-shell holes also exhibit a similarly fast de-excitation (see fig. 2(a)). We present in the following a discussion on the suppression of the ions auto-ionization by energy release to neighbouring target atoms, i.e. ICD (see 1(b)).

Slow highly charged ions are produced in an electron beam ion trap from Dreebit, Germany. Ions are extracted by means of electrostatic fields and charge state selected by an analyzing magnet. The ions are decelerated by an electrostatic retarding potential in front of a target chamber to energies between 10 and 150 keV. The pressure in the ion source, beam-line, and target chamber is kept well below 5×10^{-9} mbar to avoid charge exchange of the ions with residual gas. Graphene samples are grown by standard CVD on Cu foils and transferred without use of a polymer coating. The graphene layer is put on a TEM grid with a Quantifoil support. Ions are transmitted through graphene or are stopped within the Quantifoil. Thus, we only measure ions which have interacted with graphene or those which go through uncovered Quantifoil holes. Ion detection takes place about 20 cm (time-of-flight > 400 ns) behind the sample in an electrostatic analyzer. The analyzer allows charge state and energy measurements with a relative energy resolution of about 5×10^{-3}.

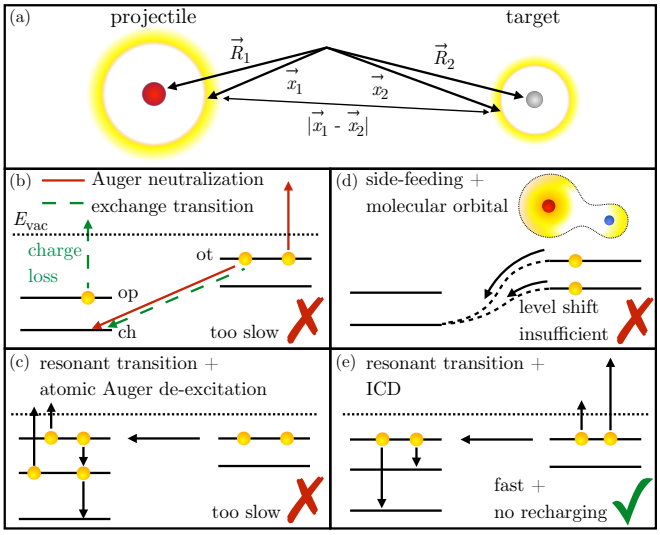

FIG. 3. (color online) (a): Projectile and target coordinates. (b): Auger neutralization and exchange transition. (c): Atomic Auger de-excitation and resonant resupply of electrons. (d): Electron side-feeding and molecular orbital formation. (e): ICD.

Experimental results are compared to predictions from a model assuming a purely atomic de-excitation cascade of a hollow Xe atom and from a model including electronic level interaction during ion collision. The details of the calculations can be found in the Supplementary Information (SI). Additionally we calculated the electronic structure and subsequently the binding energies of ionic levels for strongly ionized Xe by means of the full-potential electronic structure calculation method [22] as well as the evolution of molecular orbitals for a Xe-C pair based on the DFT code x2dhf [23].

Our ion-target system offers important features such as very asymmetric scattering partners, i.e. a heavy ion and a light target; a dense atomic environment of the target atoms; a high projectile charge, i.e. deep lying core holes; and finally a low ion velocity enabling ICD processes to take place.

Charge state distributions of Ar^{16+} and Xe^{30+} ions are depicted in fig. 2(a) for ions transmitted through

graphene. The number of stabilized electrons is determined by the difference between the incident charge state and the exit charge states. For the two ion incident charge states shown in fig. 2(a) we also used two different kinetic energies and thus varied the interaction time with the graphene sheet between 1.4 and 3.6 fs (see SI). For all ions the mean number of electrons stabilized in the ion projectile is large, especially in light of the short interaction time. We calculate a neutralization time constant τ_n for charge states investigated here, confirming an exponential dependence of the number of captured electrons on the interaction time [21]. The charge state dependence of τ_n is shown in fig. 2(b). The projectile is entirely neutralized after about 3-7 fs. The capture of a large number of electrons is certainly not surprising and was shown in many studies of the last two decades [8–11]. However, the data in fig. 2(a) can only be explained if the charge capture *as well as* the de-excitation of the captured electrons happens within the interaction time due to the absence of auto-ionization.

In general four types of processes can lead to ion de-excitation within the short interaction time: (i) Auger neutralization [14], (ii) side-feeding [8, 24], (iii) resonant capture and enhanced atomic Auger decay [25, 26] and (iv) ICD [27, 28] (see fig. 3(b)-(e)). We will show that the first three processes are associated with rates of $10^{11} - 10^{12}\,\mathrm{s}^{-1}$ (time constant of 1-10 ps), whereas our experimental results can only be explained by ICD with a rate in the order of $10^{15}\,\mathrm{s}^{-1}$ or above (time constant of 1 fs).

(i) Auger neutralization (also known as electron transfer mediated decay [29, 30]) is a process by which an electron is transferred from the target material into a deeply bound projectile state [14]. The excess energy is released by emission of a target electron (see fig. 3(b)). This process is very similar to the *exchange transition* [27] by which a target electron is captured into a deeply bound projectile state and a projectile electron is emitted (see SI). Core holes discussed here are states in a highly charged ion which are some hundred eV to keV deep in binding energy and their spatial extent is small. In fact, the wave function overlap between an outer target electron and the core orbital is small. The same argument holds for other kinds of interatomic Auger processes [29–31]. The corresponding rates of Auger neutralization and exchange transition are at least 2 - 3 orders of magnitude too small, i.e. in the range of only $10^{11} - 10^{12}\,\mathrm{s}^{-1}$ [28–30].

(ii) Side-feeding is a charge transfer concept which is similar to resonant charge transfer (described above in case of above-surface-transport) and occurs at close target-projectile encounters [6, 32]. Here electrons are transferred from deep target levels resonantly into deep ion levels (see fig. 3(d)). In this case the ion de-excites, loses its outer electrons and leaves the target with core holes. In our asymmetric target-projectile system this process is ineffective, because valence electrons are too high in energy and carbon core electrons are only two per atom and still too high in energy (285 eV). Binding energies for $n = 6 - 13$ levels of xenon ions in charge states up to 20 are shown in fig. 4(a), whereas even lower levels with $n = 3 - 5$ must be occupied from captured electrons when reaching the atomic ground state. To enhance the efficiency of this process one can think of molecular orbitals formed during the collision (see fig. 3(d)). They would promote deep projectile levels and demotes high target levels thus side-feeding may be possible again (quasi-resonance) [24, 33]. To check this we calculated molecular orbitals for xenon and carbon at several interatomic distances, shown in fig 4(b). Only carbon valence states mix with outer xenon levels. Deep xenon levels are essentially not affected by the collision. Especially in a highly charged xenon ion where the shells are even stronger bound (see fig. 4(a)) the effect of molecular orbital formation will be completely absent.

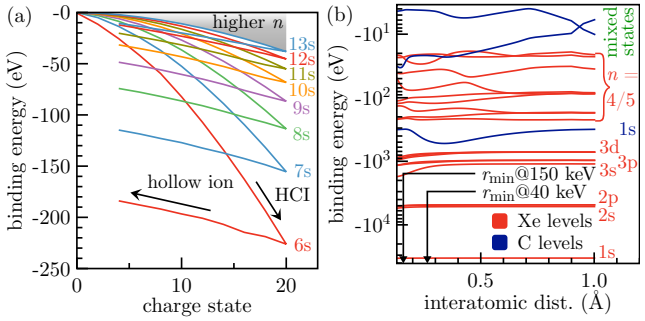

FIG. 4. (color online) (a): All electronic states of Xe get strongly demoted as function of charge state and higher principal quantum numbers n become binding. If the Xe ion captures electrons into high Rydberg states inner shells become slightly promoted again (hollow ion/atom formation). (b): Electron binding energies for a quasi-molecule of neutral xenon and carbon as function of the interatomic distance.

(iii) Resonant capture and enhanced atomic Auger rates would still explain the number of stabilized electrons from the graphene valence electrons occupying ion states with binding energies of 5-25 eV [17]. These electrons may de-excite in the ion radiatively or non-radiatively [6]. Radiative decay is associated with decay times in the nanosecond range [30, 34] (only for K and L shell filling rates of $10^{14}\,\mathrm{s}^{-1}$ may be possible [34]). The non-radiative Auger-type auto-ionization will therefore account for a significant part of the de-excitation sequence [6, 14]. The electrons lost by this process must be refilled from graphene as sketched in fig. 3(c), otherwise only a few (1-5) electrons remain stabilized in the ion subsequent to the entire cascade [11]. Resupply of electrons during the short interaction time must involve the frequently made assumption of enhanced atomic Auger rates in hollow atoms [9, 10]. To check for this enhancement we used a state-of-the-art relativistic atomic structure code MCDFGME [35, 36] and calculated Auger transition rates for

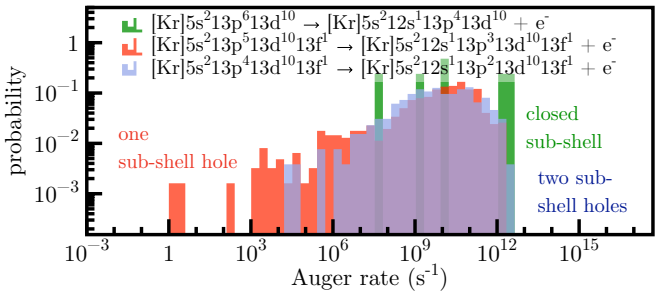

FIG. 5. (color online) Atomic Auger rates for three specific hollow atom configurations shown as a histogram with probability of occurrence.

specific hollow atom configurations with occupied principal quantum numbers up to $n = 13$. We find rates in the order of $10^8 - 10^{12}\,\mathrm{s}^{-1}$ which are not enhanced (see fig. 5). Only for innershell transitions, i.e. at smaller $n = 1, 2$ or 3, rates increase to $10^{14} - 10^{15}\,\mathrm{s}^{-1}$ [34, 37, 38]. In our case rates in the order of $10^{15} - 10^{17}\,\mathrm{s}^{-1}$ for $n > 10$ are necessary [21] for the *entire* cascade to succeed within the interaction time. Due to this large discrepancy we exclude also enhanced atomic Auger rates as the origin for the observed fast electronic decay.

(iv) Finally an ultrafast electronic decay process allowing *energy* transfer to the target without *electron* transport is the only channel left. ICD is a de-excitation mechanism which involves the filling of a core hole by a valence electron of the *same* atom and the promotion of a valence electron of a *neighbouring* atom into the continuum (see fig. 3(e)) [12, 27]. Commonly ICD is discussed only in weakly bound systems, such as van-der-Waals systems. This is due to necessary electron-electron interaction of the outer electrons (of neighbouring atoms) which is only strong enough if the electronic orbitals have large extent. In our case the projectile is a hollow atom with many occupied Rydberg orbitals ($n > 20$) and its distance of closest approach ($0.2 - 1.4\,\text{Å}$) to a target atom is much smaller than typical equilibrium distances in a van-der-Waals system ($\gtrsim 3\,\text{Å}$). Hence, ICD is very well active in our collisional system.

ICD (also known as direct Auger *de-excitation*) has gained attention due to its importance in photoionization processes of molecules embedded in a liquid environment [12, 27, 39, 40]. ICD still describes Coulomb scattering of target and projectile electrons which makes it hard to estimate the lifetime dependence on the interatomic distance $R = \left|\vec{R}_1 - \vec{R}_2\right|$. Both target and (Rydberg-like) projectile electrons have large spatial extent and thus may interact over large distances ($1/R$ dependence). Since we assume not only the nearest carbon neighbors of the impacting xenon and argon ion to participate in the ICD, contributions of next-nearest neighbours should be taken into account. For their contribution Santra *et al.* derived a $1/R^6$ dependence [29] in the so-called virtual photon model, which makes ICD with next-nearest neighbours a local process only present at small impact parameters of our ions. A more sophisticated treatment of the distance dependence based on the Greens function method includes effects of the electron wave function overlap at close distances [30]. This method revealed an even stronger enhancement of the decay rate for small distances. In fact, an extrapolation of the calculated rates/decay width by Averbukh and Cederbaum for asymmetric MgNe and CaNe dimers shows a decay time constant of about 3 fs at $R = 1 - 2\,\text{Å}$ [30]. Recently we already showed that at these small impact parameters a new charge exchange mechanism distinctly different from cases (i)-(iii) is present [11].

In addition it was shown that the rate of ICD depends strongly on the number of nearest neighbours or the cluster size [41, 42]. For Neon clusters a strong lifetime (1/rate) reduction well below 1 fs was calculated for clusters containing up to 13 atoms [29]. It may even be smaller than 1 fs in a macromolecule such as graphene. Since in our case the entire de-excitation sequence by ICD including most of the captured electrons (up to 30 depending on the initial charge state, see fig. 2(a)) is finished within 7 fs [21] it is fair to assume a large contribution of next-nearest and even farther neighbours. Yet, ICD within a solid surface is not infinitely fast, since we see a clear time dependence of the neutralization dynamics when varying the ion kinetic energy (see fig. 2(a)). By doing so we experimentally determine a time constant τ_n for both resonant charge transfer (step 1) and ICD (step 2) depicted in fig 1(a) and (b) to take place according to $\bar{N}_\mathrm{stab} \equiv Q_\mathrm{in} - \bar{Q}_\mathrm{out} = Q_\mathrm{in}\left(1 - e^{-t/\tau_\mathrm{n}}\right)$ with the mean number of stabilized electrons $\bar{N}_\mathrm{stab}$ and the incident and mean exit charge states Q_in and $\bar{Q}_\mathrm{out}$, respectively, as well as the time t. The time constant depends on the ion charge state Q_in with values of a few femtoseconds (see fig. 2(b)) well in agreement with distance and cluster size dependent values reported in literature [28–30, 41] and discussed above. This value is an upper bound for the ICD lifetime, because it is averaged over ion-target distances of $\sim 1\,\text{Å}$ (distance of closest approach) to $\sim 10\,\text{Å}$ (distance of first charge transfer).

ICD also predicts slow electron emission from the neighbouring atoms which then carry part of the excitation energy. Electron emission from surfaces triggered by projectile de-excitation was previously measured directly showing that the yield γ is about 2-3 times the incident charge state ($\gamma = 200$ electrons/ion for Th^{79+} on clean Au(111) [43, 44]), the mean of the energy distribution is below 20 eV [45, 46], and emitted electrons can even be correlated[47]. These facts are well in agreement with an ICD process. For 263 keV Xe^{30+} ions we have now directly measured the electron yield from graphene in coincidence with ions transmitted in charge states $Q < 30$, i.e. for ions which have passed the graphene layer. As a results we find $\gamma_\mathrm{graphene} \approx 21$ electrons/ion with an esti-

mated collection efficiency of $28 \pm 5\%$. This yield (corrected by efficiency $\gamma_{\mathrm{corr}} \approx (75 \pm 20)$ electrons/ion) is remarkably high considering only a single layer of carbon atoms.

In conclusion we determined experimentally neutralization and de-excitation time constants of highly charged ions of about 1-3 fs. We find evidence that HCI neutralize by hollow atom formation and the subsequent de-excitation is mainly driven by ICD. Further evidence for ICD is presented by the measured emission of > 20 electrons per impacting ion.

Financial support by the Deutsche Forschungsgemeinschaft (WI 4691/1-1), the Austrian FWF (I1114-N20), and the TU-D doctoral college of TU Wien is gratefully acknowledged. R.K. and M.S. are grateful for support from SFB 1242 "Non-Equilibrium Dynamics of Condensed Matter in the Time Domain" and SPP 1459 "Graphene".

* Author to whom correspondence should be addressed. Electronic mail: r.wilhelm@hzdr.de

[1] U. Littmark and P. Sigmund, J. Phys. D-Applied Phys. **8**, 241 (1975).
[2] A. S. El-Said, R. Heller, W. Meissl, R. Ritter, S. Facsko, C. Lemell, B. Solleder, I. C. Gebeshuber, G. Betz, M. Toulemonde, W. Möller, J. Burgdörfer, and F. Aumayr, Phys. Rev. Lett. **100**, 237601 (2008).
[3] B. Liedke, K.-H. Heinig, and W. Möller, Nucl. Instruments Methods Phys. Res. Sect. B Beam Interact. with Mater. Atoms **316**, 56 (2013).
[4] R. A. Wilhelm, A. S. El-Said, F. Krok, R. Heller, E. Gruber, F. Aumayr, and S. Facsko, Prog. Surf. Sci. **90**, 377 (2015).
[5] R. A. Wilhelm and W. Möller, Phys. Rev. A **93**, 052709 (2016).
[6] A. Arnau, F. Aumayr, P. Echenique, M. Grether, W. Heiland, J. Limburg, R. Morgenstern, P. Roncin, S. Schippers, R. Schuch, N. Stolterfoht, P. Varga, T. Zouros, and H. Winter, Surf. Sci. Rep. **27**, 113 (1997).
[7] R. Herrmann, C. L. Cocke, J. Ullrich, S. Hagmann, M. Stäckli, and H. Schmidt-Böcking, Phys. Rev. A **50**, 1435 (1994).
[8] S. Winecki, C. L. Cocke, D. Fry, and M. P. Stöckli, Phys. Rev. A **53**, 4228 (1996).
[9] T. Schenkel, A. Hamza, A. Barnes, and D. Schneider, Prog. Surf. Sci. **61**, 23 (1999).
[10] S. Martin, R. Brédy, J. Bernard, J. Désesquelles, and L. Chen, Phys. Rev. Lett. **89**, 183401 (2002).
[11] R. A. Wilhelm, E. Gruber, R. Ritter, R. Heller, S. Facsko, and F. Aumayr, Phys. Rev. Lett. **112**, 153201 (2014).
[12] L. S. Cederbaum, J. Zobeley, and F. Tarantelli, Phys. Rev. Lett. **79**, 4778 (1997).
[13] H. S. W. Massey and R. H. Fowler, Math. Proc. Cambridge Philos. Soc. **26**, 386 (1930).
[14] H. D. Hagstrum, Phys. Rev. **96**, 336 (1954).
[15] S. Marburger, O. Kugeler, U. Hergenhahn, and T. Möller, Phys. Rev. Lett. **90**, 203401 (2003).
[16] T. Jahnke, A. Czasch, M. S. Schöffler, S. Schössler, A. Knapp, M. Käsz, J. Titze, C. Wimmer, K. Kreidi, R. E. Grisenti, A. Staudte, O. Jagutzki, U. Hergenhahn, H. Schmidt-Böcking, and R. Dörner, Phys. Rev. Lett. **93**, 163401 (2004).
[17] J. Burgdörfer, P. Lerner, and F. W. Meyer, Phys. Rev. A **44**, 5674 (1991).
[18] J. P. Briand, L. de Billy, P. Charles, S. Essabaa, P. Briand, R. Geller, J. P. Desclaux, S. Bliman, and C. Ristori, Phys. Rev. Lett. **65**, 159 (1990).
[19] H. Winter and F. Aumayr, J. Phys. B At. Mol. Opt. Phys. **32**, R39 (1999).
[20] M. Hattass, T. Schenkel, A. V. Hamza, A. V. Barnes, M. W. Newman, J. W. McDonald, T. R. Niedermayr, G. A. Machicoane, and D. H. Schneider, Phys. Rev. Lett. **82**, 4795 (1999).
[21] E. Gruber, R. A. Wilhelm, R. Pétuya, V. Smejkal, R. Kozubek, A. Hierzenberger, B. C. Bayer, I. Aldazabal, A. K. Kazansky, F. Libisch, A. V. Krasheninnikov, M. Schleberger, S. Facsko, A. G. Borisov, A. Arnau, and F. Aumayr, Nat. Commun. **7**, 13948 (2016).
[22] J. M. Wills, M. Alouani, P. Andersson, A. Delin, O. Eriksson, and A. Grechnev, *Full-Potential Electronic Structure Method, Energy and Force Calculations with Density Functional and Dynamical Mean Field Theory*, Springer Series in Solid-State Sciences, Vol. 167 (Springer-Verlag, Berlin Heidelberg, 2010).
[23] J. Kobus, Comput. Phys. Commun. **184**, 799 (2013).
[24] N. Stolterfoht, A. Arnau, M. Grether, R. Köhrbrück, A. Spieler, R. Page, A. Saal, J. Thomaschewski, and J. Bleck-Neuhaus, Phys. Rev. A **52**, 445 (1995).
[25] N. Vaeck, J. E. Hansen, P. Palmeri, P. Quinet, N. Zitane, M. Godefroid, S. Fritzsche, and N. Kylstra, Phys. Scr. **T95**, 68 (2001).
[26] P. Palmeri, P. Quinet, N. Zitane, and N. Vaeck, J. Phys. B At. Mol. Opt. Phys. **34**, 4125 (2001).
[27] T. Jahnke, J. Phys. B At. Mol. Opt. Phys. **48**, 082001 (2015).
[28] J. Rist, T. Miteva, B. Gaire, H. Sann, F. Trinter, M. Keiling, N. Gehrken, A. Moradmand, B. Berry, M. Zohrabi, M. Kunitski, I. Ben-Itzhak, A. Belkacem, T. Weber, A. Landers, M. Schöffler, J. Williams, P. Kolorenč, K. Gokhberg, T. Jahnke, and R. Dörner, Chem. Phys. , 1 (2016).
[29] R. Santra, J. Zobeley, and L. Cederbaum, Phys. Rev. B **64**, 245104 (2001).
[30] V. Averbukh and L. S. Cederbaum, J. Chem. Phys. **123**, 204107 (2005).
[31] J. Matthew and Y. Komninos, Surf. Sci. **53**, 716 (1975).
[32] L. Folkerts, S. Schippers, D. M. Zehner, and F. W. Meyer, Phys. Rev. Lett. **74**, 2204 (1995).
[33] A. Arnau, R. Köhrbrück, M. Grether, A. Spieler, and N. Stolterfoht, Phys. Rev. A **51**, R3399 (1995).
[34] R. Díez Muiño, A. Salin, N. Stolterfoht, A. Arnau, and P. M. Echenique, Phys. Rev. A **57**, 1126 (1998).
[35] J. Desclaux, Comput. Phys. Commun. **9**, 31 (1975).
[36] P. Indelicato and J. P. Desclaux, Phys. Rev. A **42**, 5139 (1990).
[37] C. P. Bhalla, Phys. Rev. A **8**, 2877 (1973).
[38] N. Vaeck and J. E. Hansen, Zeitschrift für Phys. D Atoms, Mol. Clust. **21**, S221 (1991).
[39] S. Thürmer, M. Ončák, N. Ottosson, R. Seidel, U. Hergenhahn, S. E. Bradforth, P. Slavíček, and B. Winter, Nat. Chem. **5**, 590 (2013).
[40] K. Gokhberg, P. Kolorenč, A. I. Kuleff, and L. S. Ceder-

baum, Nature **505**, 661 (2013).
[41] G. Öhrwall, M. Tchaplyguine, M. Lundwall, R. Feifel, H. Bergersen, T. Rander, A. Lindblad, J. Schulz, S. Peredkov, S. Barth, S. Marburger, U. Hergenhahn, S. Svensson, and O. Björneholm, Phys. Rev. Lett. **93**, 173401 (2004).
[42] Y. Ovcharenko, V. Lyamayev, R. Katzy, M. Devetta, A. LaForge, P. O'Keeffe, O. Plekan, P. Finetti, M. Di Fraia, M. Mudrich, M. Krikunova, P. Piseri, M. Coreno, N. B. Brauer, T. Mazza, S. Stranges, C. Grazioli, R. Richter, K. C. Prince, M. Drabbels, C. Callegari, F. Stienkemeier, and T. Möller, Phys. Rev. Lett. **112**, 073401 (2014).
[43] H. Kurz, K. Töglhofer, H. Winter, F. Aumayr, and R. Mann, Phys. Rev. Lett. **69**, 1140 (1992).
[44] F. Aumayr, H. Kurz, D. Schneider, M. A. Briere, J. W. McDonald, C. E. Cunningham, and H. Winter, Phys. Rev. Lett. **71**, 1943 (1993).
[45] R. Köhrbrück, K. Sommer, J. P. Biersack, J. Bleck-Neuhaus, S. Schippers, P. Roncin, D. Lecler, F. Fremont, and N. Stolterfoht, Phys. Rev. A **45**, 4653 (1992).
[46] D. Kost, S. Facsko, W. Möller, R. Hellhammer, and N. Stolterfoht, Phys. Rev. Lett. **98**, 225503 (2007).
[47] C. H. Li, C. Tusche, F. O. Schumann, and J. Kirschner, Phys. Rev. Lett. **118**, 136402 (2017).